

## Impact of Some Simplifying Assumptions in the New ECMWF Surface Scheme

B. J. J. M. VAN DEN HURK\*

*Department of Meteorology, Agricultural University, Duivendaal, Wageningen, the Netherlands*

A. C. M. BELJAARS

*Royal Netherlands Meteorological Institute, De Bilt, the Netherlands*

(Manuscript received 22 May 1995, in final form 11 December 1995)

### ABSTRACT

Two simplifying assumptions adopted in the current ECMWF surface scheme are explored: a uniform skin temperature for all grid-box fractions with variable latent heat release and a fixed value of an effective heat conductivity defining the soil heat flux density. This paper proposes relatively simple modifications of the ECMWF scheme with a better physical basis, without large input or computer infrastructure requirements.

A uniform skin temperature overestimates evaporation from relatively wet surface fractions when the other surface components are dry and warm. This is shown to be the case for an evaporating soil after rain and vegetation evaporation in a sparse Mediterranean vineyard canopy. Allowing different temperatures for each surface fraction significantly reduces the overestimations and introduces only little additional computation.

The default effective conductivity value ( $7 \text{ W m}^{-2} \text{ K}^{-1}$ ) employed by the current ECMWF scheme is shown to be too low for the sparse vineyard canopy. By raising the conductivity to  $17 \text{ W m}^{-2} \text{ K}^{-1}$  for the bare-soil part of the surface, the daytime simulated soil heat flux was improved considerably.

### 1. Introduction

Numerical models for the atmosphere are operated widely for the prediction of daily weather or for studies of the impact of human activities on regional or global climate. As a lower boundary condition, these models use a parameterization scheme for the exchange of heat, scalars, and momentum at the surface.

Recently, Viterbo and Beljaars (1995, VB95 hereafter) introduced a new surface scheme for the operational global model of the European Centre for Medium-Range Weather Forecasts (ECMWF). Embedded in a global model, the surface scheme is designed to describe the surface fluxes over a wide range of possible vegetation covers and timescales. In order to avoid excessive data and computational requirements, it is sometimes necessary to simplify the parameterization of the transfer of scalars and momentum to and from the surface.

One of the simplifications included in their scheme was the representation of the surface by a single layer with uniform temperature. This layer is referred to as

a "skin layer." Four different grid-box fractions with respect to evaporation are accounted for: bare soil, dry vegetation, an open water reservoir filled with dew and intercepted water, and snow. The evaporation rate of each of these fractions is computed using a humidity gradient between a reference level and the surface. For the interception reservoir and the vegetation, the surface humidity is assumed to be saturated at surface temperature. For the bare ground, a relative humidity is used that is a function of the soil moisture content of the top soil layer.

In practice, the temperature of a nonuniformly vegetated surface can exhibit large differences between, for example, the vegetation and the bare-soil component of the surface. Under conditions of a well-watered vegetation stand only partially covering the surface and high sensible heat release by the bare ground, adopting a single surface temperature for both the vegetation and the bare ground can lead to a significant overestimation of the canopy evaporation rate. Also, the predicted bare-soil evaporation rate is often strongly overestimated for a few hours after a period with rain, when a canopy is also present. The temperature of the canopy component rapidly increases once the intercepted water is evaporated, and this temperature increase unrealistically enhances the simulated evaporation rate of the bare ground.

A second simplification employed by VB95 is the use of an empirical effective conductivity for heat transfer through the skin layer. This skin conductivity

\* Also affiliated with Royal Netherlands Meteorological Institute, De Bilt, the Netherlands.

Corresponding author address: Mr. B. J. J. M. van den Hurk, KNMI, P.O. Box 201, 3730 AE De Bilt, the Netherlands.

$\Lambda$  ( $\text{W m}^{-2} \text{K}^{-1}$ ) is defined as the ratio between the ground heat flux and the temperature difference between the top soil layer and the skin layer. A uniform value of  $7 \text{ W m}^{-2} \text{K}^{-1}$  was chosen as to realize a reasonable amplitude of the diurnal cycle of the ground heat flux, following Beljaars and Betts (1992), who used grassland data taken at the meteorological observation station in Cabauw, the Netherlands.

The physical interpretation of  $\Lambda$  is to express the efficiency of the heat flow through the vegetation layer and the top soil layer. When the surface consists of a completely bare soil, the empirical parameter  $\Lambda$  can be related to a physical soil thermal conductivity. When a dense vegetation cover is present, the heat flow into the soil and vegetation layer will also be affected by the turbulent heat exchange within the vegetation layer. Skin conductivity  $\Lambda$  then also incorporates the effect of the thermal isolation by the canopy cover on the soil heat flow. A detailed discussion about the physical interpretation for  $\Lambda$  and the validity of the choice for its (uniform) value is discussed below.

The two simplifications mentioned here are obviously dictated by the severe constraints on global input data, computer time, and the possibility to modify model components in an operational environment. However, as will be shown in this paper, it is possible to derive alternative formulations to these simplifications, which increase the physical base of the surface scheme, in particular for cases where the surface vegetation cover is sparse. Simultaneously, the need for additional data input or major changes to model infrastructure is avoided.

It is the aim of this paper to explore the implications of the original and the new formulations for the skin temperature and skin conductivity. For this, data from two large-scale field experiments are used: FIFE (Sellers et al. 1988) and EFEDA (Bolle et al. 1993). Attention is paid to the realism of the description of surface energy balance by the original and modified scheme. In order to indicate the implications for weather prediction purposes, long-term simulations of the cumulative evaporation are compared to available field measurements from both experiments. First, we will pay attention to the issue of the uniform skin layer temperature, followed by a discussion of the skin conductivity.

## 2. The skin-layer temperature

The scheme of VB95 solves the surface temperature  $T_s$  implicitly by considering the energy balance of the surface:

$$(1 - a)R_s + (1 - \epsilon)R_T - \epsilon\sigma T_s^4 - H - LE = \Lambda(T_s - T_1). \quad (1)$$

Here  $a$  is the shortwave albedo,  $R_s$  and  $R_T$  the downward shortwave and longwave radiation,  $\epsilon$  the surface

longwave emissivity,  $H$  the sensible heat flux,  $LE$  the latent heat flux,  $\Lambda$  the skin conductivity, and  $T_1$  the temperature of the first soil layer, which has a depth of 0.07 m. The radiative fluxes are defined positive toward the surface, while  $H$ ,  $LE$ , and  $G$  are defined positive from the surface. The soil heat flux  $G$  is given by

$$G = \Lambda(T_s - T_1). \quad (2)$$

The total sensible and latent heat fluxes  $H$  and  $LE$  are specified according to

$$H = \rho C_H u_L (C_p T_s - C_p T_L - g z_L) \quad (3)$$

and

$$LE = L\rho [a_s q_{\text{sat}}(T_s) - a_L q_L], \quad (4)$$

where  $u_L$  is the wind speed at reference level  $z_L$  (the lowest model level in the large-scale model),  $C_H$  the stability dependent transfer coefficient between the surface and the reference height (Beljaars and Holtlag 1991),  $\rho$  the air density,  $C_p$  the specific heat of dry air,  $g$  the gravity acceleration,  $q_L$  and  $T_L$  the specific humidity and temperature at reference level,  $q_{\text{sat}}$  the saturation specific humidity,  $L$  the latent heat of vaporization, and  $a_L$  and  $a_s$  coefficients dependent on the relative fractions in the grid box, to be specified subsequently. If  $C_v$  is the fraction of the grid box covered with vegetation and  $C_l$  the fraction covered with water in the interception reservoir due to dew or precipitation, the total evaporation is expressed according to

$$E = C_l E_l + (1 - C_l) C_v E_v + (1 - C_l)(1 - C_v) E_g, \quad (5)$$

where  $E_l$  is the evaporation from the interception reservoir,  $E_v$  the evaporation from the vegetation, and  $E_g$  the bare ground evaporation.<sup>1</sup> Coefficients  $a_L$  and  $a_s$  depend on the relative area and the different resistances to evaporation of each fraction, according to

$$a_L = \frac{C_l}{r_a} + \frac{(1 - C_l)C_v}{r_a + r_c} + \frac{(1 - C_l)(1 - C_v)}{r_a} \quad (6)$$

and

$$a_s = \frac{C_l}{r_a} + \frac{(1 - C_l)C_v}{r_a + r_c} + \frac{\alpha(1 - C_l)(1 - C_v)}{r_a}, \quad (7)$$

where  $r_a$  is the aerodynamic resistance (given by  $1/u_L C_H$ ),  $r_c$  the canopy resistance for evaporation, and  $\alpha$  the relative humidity of the top soil, which is a function of the soil moisture content of the upper soil layer.

Equation (1) is solved by linearizing  $T_s^4$  using a Taylor expansion and  $q_{\text{sat}}(T_s)$  using a value of  $\partial q_{\text{sat}}/\partial T$  at

<sup>1</sup> The effects of snow are not considered here since it was not included in the datasets we used.

the value of  $T_s$  of the previous time step. An iterative scheme is used to account for the stability correction of  $C_H$ . The ECMWF scheme uses  $C_H$  from the previous time step explicitly and an implicit solver for the temperature at the new time level (Beljaars 1992).

Obviously, the values for  $T_s$  found from (1)–(7) will depend on the relative surface fractions covering the grid box. When the canopy resistance differs from 0 and the relative humidity at the soil surface is less than 1,  $T_s$  will depend on  $C_l$  and  $C_v$ . For instance, with  $C_l = 1$  the entire grid box has a wet interception reservoir, and the skin temperature will adjust to a potential evaporation rate ( $r_c \rightarrow 0$ ,  $\alpha \rightarrow 1$ ).

In order to avoid the unrealistic coupling between different surface fractions (e.g., bare soil and vegetation) through a single skin temperature, it is necessary to allow this skin temperature to be different for the bare soil, the vegetation, and wet surface fractions. Once the vegetation temperature is allowed to differ from the bare-ground temperature, excessive canopy evaporation under dry conditions is readily avoided. In practice, vegetation can remain much cooler than bare ground because it can sustain evaporation by accessing water from deeper soil layers. Multiple source models, as presented for instance by Dolman (1993), allow for these temperature differences by using the Penman–Monteith concept (Monteith 1981) separately for the canopy elements and the underlying soil.

Our proposed strategy to allow for different surface temperatures for the different components is to calculate the surface energy balance using (1) separately for each component. The final grid-box-averaged energy flux is then computed from the energy fluxes and temperatures from each component according to the same weighing scheme as presented in (5). The separate energy balance solutions are calculated in a straightforward manner by selecting appropriate values for  $a_l$  and  $a_s$ . The surface energy balance of the interception reservoir is obtained by calculating  $a_l$  and  $a_s$  by (6) and (7) and taking  $C_l = 1$ . The energy balance and the associated surface temperature for the vegetation component is obtained by choosing  $C_l = 0$  and  $C_v = 1$ . Finally, the bare soil temperature results from a solution of the energy balance equation by taking  $C_l = C_v = 0$ .

As in the original VB95 model, the transfer from the different surface fractions is computed independently. Stated differently, horizontal exchange of heat or moisture between the various grid-box fractions is not incorporated. The independent treatment of surface fractions is reasonable if the surface fractions are large enough to have internal boundary layers that do not merge below the lowest model level. For patchy surfaces with small horizontal scales, it would be necessary to introduce an extra node in the resistance network somewhere between the surface and the lowest model level (Blyth 1995), but such a concept is diffi-

cult to handle in a global model without appropriate datasets.

To apply this proposed strategy practically, two issues need further attention: the stability dependence of  $C_H$  and the solution of the surface temperature from the linearization around the previous time step. When additional storage of parameter values between subsequent time steps should be avoided, only the average skin-layer temperature can be transferred to the next time step. Since temperature differences between the various surface components may be large, this average skin temperature is a poor estimator for linearization of  $\partial q_{\text{sat}}/\partial T$ . Also the stability correction of  $C_H$  for a specific grid-box fraction will have to be carried out using an average sensible heat flux from the previous time step, which may be rather different from the sensible heat flux in that grid-box fraction. In order to reduce the errors involved with the use of the average parameters from the previous time step, we will calculate  $C_H$  and  $\partial q_{\text{sat}}/\partial T$  by means of two iterations for each surface fraction, initialized by the average skin temperature and average sensible heat flux from the previous time step. In the appendix it is shown that two iterations gives accurate results.

### 3. Case studies for the temperature differentiation

Two case studies demonstrate the effect of discerning between the different grid-box fraction temperatures: a case regarding a drying surface after rain (measurements from FIFE) and the simulation of a series of diurnal courses of the evaporation of a sparse vineyard canopy surface (measurements taken during EFEDA).

#### a. A drying surface after rain

The original model of VB95 was validated with several datasets, including the data collected during the FIFE 1987 experiment (Sellers et al. 1988). During this experiment micrometeorological parameters were measured during 168 days, from May until October 1987. Data were collected above a tallgrass prairie in rolling terrain. Half-hourly averages of temperature, wind speed, and air humidity at reference height, as well as incoming longwave and shortwave radiation, are available. During four intensive field campaigns (IFCs), eddy correlation data of sensible and latent heat flux density were collected, together with net radiation and soil heat flux density. The observations from all available stations were averaged to obtain a single time series by Betts and Ball (1992).

Both the original and the modified scheme were used to simulate the surface fluxes for the entire experimental period. All model settings (including soil type and root profile) were taken as in the VB95 paper. Values of some surface specific parameters can be found in Table 1. The soil moisture profile was initialized at field capacity, and a vertically uniform temperature profile was taken as the initial profile.

TABLE 1. Surface parameters for the FIFE 1987 test case.

| Parameter                                | Symbol     | FIFE           | EFEDA        |
|--|------------|----------------|--------------|
| Roughness length for momentum            | $z_{0m}$   | 0.3 m          | 0.01–0.06    |
| Roughness length for heat                | $z_{0h}$   | 0.03 m         | $z_{0m}/200$ |
| Surface fraction covered with vegetation | $C_v$      | 0.85           | 0.05–0.15    |
| Surface albedo                           | $a$        | 0.168          | 0.29         |
| Longwave emissivity                      | $\epsilon$ | 0.996          | 0.996        |
| Initial soil temperature (K)             | $T$        | 291.4          | 298.2        |
| Initial soil humidity ( $m^3 m^{-3}$ )   | $\theta_w$ | field capacity | 0.08–0.15    |

For comparison with measured fluxes, a situation is selected in which the surface is drying after a period of rain. For the present study the simulations for days 176 and 177 are chosen. Unlike the intercomparisons in VB95, we focus on diurnal variations of measured and predicted surface fluxes.

Figure 1 shows the simulated and observed total evaporation for the selected days. Precipitation is also

shown, as is the evaporation from the interception reservoir  $LE_i$ . The new scheme reduces the overestimation of  $LE$  by approximately 50%, especially for day 176. Also, the pronounced peaks caused by the evaporation from the interception reservoir are reduced, although not entirely removed.

The new solution for the surface temperature has a pronounced effect on the partitioning of the evap-

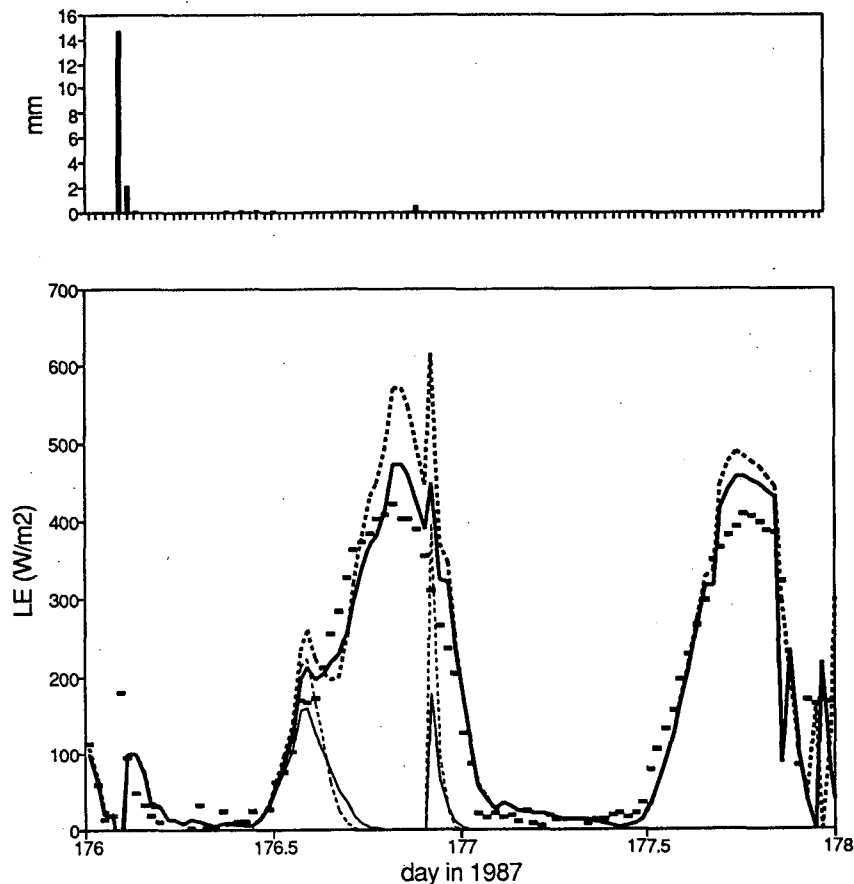


FIG. 1. Lower panel: Observed (symbols) and simulated (heavy lines) total evaporation for FIFE 1987, days 176 and 177. Simulations are carried out with both the original VB95 model (dotted lines) and the new version with different temperatures for different surface fractions (solid lines). Also shown are the simulated evaporation from the skin reservoir,  $C_i LE_i$  (thin lines), and observed precipitation (upper panel).

oration over the ground surface and the canopy. Figure 2 shows the simulated bare soil and canopy evaporation rates, given by  $(1 - C_i)(1 - C_v)LE_g$  and  $(1 - C_i)C_vLE_v$ , respectively. Since the soil is wet just after a rainy period, the bare soil evaporates at a nearly potential rate, which has a strong feedback to the surface temperature. The old scheme simulates a maximum weighted soil evaporation of about  $300 \text{ W m}^{-2}$ . For the bare ground fraction only (equal to 15% when  $C_i = 0$ ), this is equivalent to  $2000 \text{ W m}^{-2}$ ! The reason is that the dominating vegetated part imposes its higher surface equilibrium temperature on the bare soil fraction. Allowing for different temperatures of the soil and the canopy component causes a reduction of 50% of the soil evaporation, whereas the canopy evaporation is enhanced by approximately 10% around noon.

This effect is particularly present in cases of wet soils after rain events. At a seasonal timescale these events are less dominant, and the implications for the long-term moisture budget are fairly small. After 168 days of simulation, the new scheme resulted in a reduction of 5 mm on an observed total evaporation of 400 mm.

#### b. A sparsely vegetated vineyard

The model of VB95 was also run for a sparsely vegetated Mediterranean vineyard area for 60 consecutive days between 1 June and 30 July 1994. Data were collected in the Tomelloso area during the EFEDA-II intensive measurement campaign, which was a follow-up of EFEDA-I (Bolle et al. 1993). The fraction of

area covered by vegetation,  $C_v$ , increased from  $\pm 0.05$  to  $\pm 0.15$  in the considered period, and the leaf area index did not exceed  $0.25 \text{ m}^2 \text{ m}^{-2}$  (Van den Hurk 1996; see Table 1). Since dew and precipitation were absent in this period, the fraction of area covered by the interception reservoir ( $C_i$ ) was zero all time. The soil consisted of sandy loam material and the top layer was covered with stones and was very dry. The plants extracted water from deeper soil layers ( $>1 \text{ m}$ ), and canopy evaporation could be sustained in spite of the very dry top soil.

Eddy-correlation measurements of total sensible and latent heat were available, and soil heat flux was measured with soil heat flux plates buried at 1-cm depth, corrected for heat storage above the plates. Soil temperatures were measured using PT100 resistance thermometers, placed under both sunlit and shaded soil plots at 1- and 5-cm depths. Surface temperatures were obtained from an infrared sensor mounted at 8-m height. Canopy temperatures were derived from multiple leaf temperature measurements, obtained at specific days using handheld radiometric thermometers. For details on the measurements we refer to Van den Hurk (1996).

For the settings of most model parameters, the suggestions made by VB95 were followed. In the original model, the canopy resistance  $r_c$  is parameterized as function of the soil water content of the top three layers and the intercepted radiation. However, in this study an empirical expression was used, expressed as function of time. This expression was calibrated using field data of total evaporation, stomatal conductance (mea-

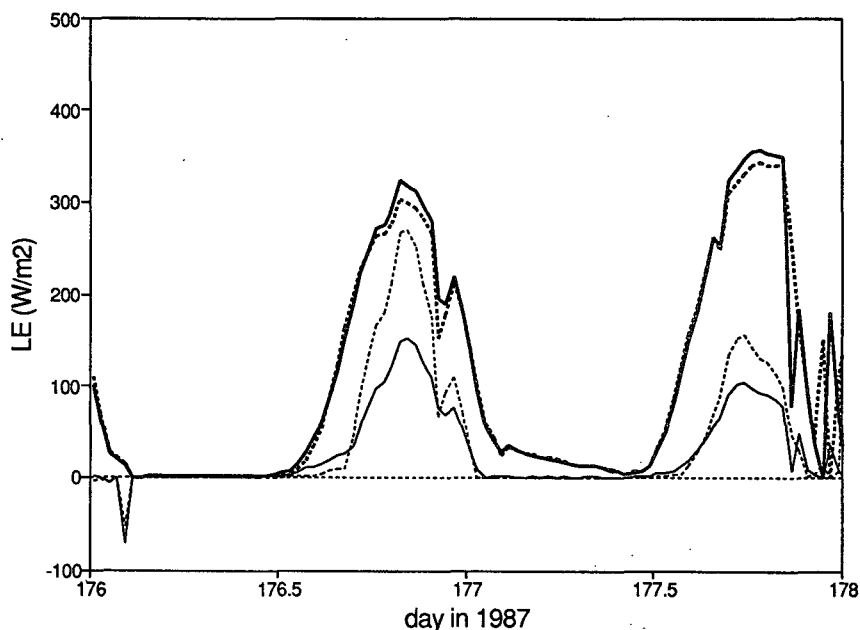


FIG. 2. Simulation of the canopy evaporation,  $(1 - C_i)C_vLE_v$  (thick lines), and soil evaporation,  $(1 - C_i)(1 - C_v)LE_g$  (thin lines), for the original model (dotted) and new version (solid).

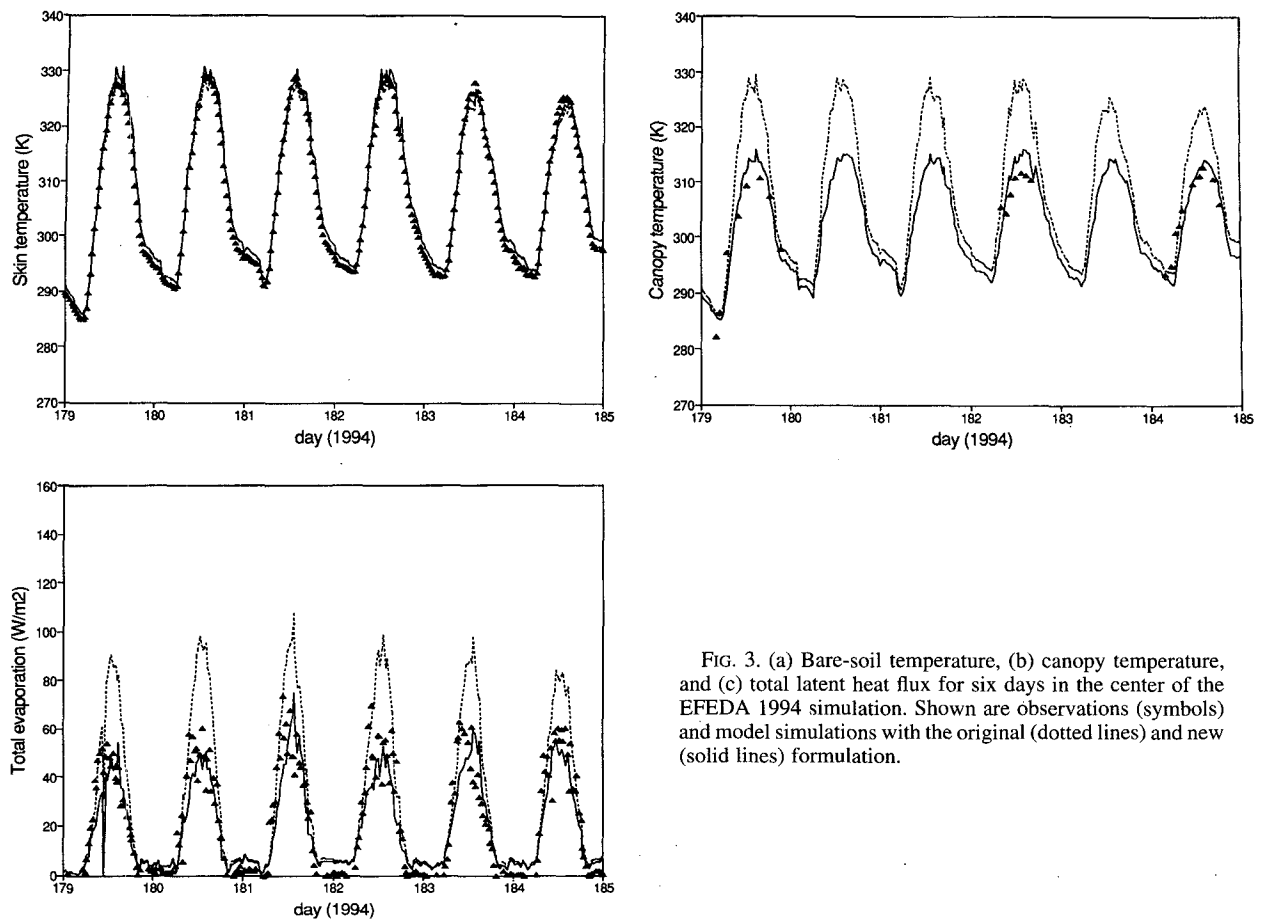


FIG. 3. (a) Bare-soil temperature, (b) canopy temperature, and (c) total latent heat flux for six days in the center of the EFEDA 1994 simulation. Shown are observations (symbols) and model simulations with the original (dotted lines) and new (solid lines) formulation.

sured between sunrise and sunset at approximately every third day during the experimental period using a dynamic diffusion porometer), leaf area index, and the fraction of surface covered with vegetation  $C_v$ . By this procedure,  $r_c$  showed a diurnal variation with a minimum value ( $r_{c,\min}$ ) around 1000 UTC. The observations of total evaporation showed a limited day-to-day variation, in spite of a significant increase of  $C_v$ . In the empirical expressions this was incorporated by keeping the ratio  $C_v/r_{c,\min}$  constant.

The physical soil parameters were quantified according to the sandy loam soil type cited by Noilhan and Planton (1989). Surface albedo was taken as 0.29 at all times, deduced from field observations. The apparent conductivity of the skin layer ( $\Lambda$ ) was taken as  $7 \text{ W m}^{-2} \text{ K}^{-1}$ , and the drag coefficient  $C_H$  was computed using  $z_{0m}/z_{0h} = 200$ , following Van den Hurk et al. (1995). These adaptations were necessary to predict a reasonable value of the surface temperature and the soil heat flux. The initial soil moisture content was estimated at  $0.13 \text{ m}^3 \text{ m}^{-3}$  for the soil layers below 30-cm depth, and  $0.04 \text{ m}^3 \text{ m}^{-3}$  near the surface. These estimates were based on simultaneous measurements taken

at a similar site nearby the experimental area (Grünwald 1995, personal communication).

Figure 3 shows observations and simulations of (a) bare-soil temperature, (b) canopy temperature, and (c) total latent heat flux for a series of six consecutive days in the center of the simulation period. Simulations with both the original and the modified scheme are shown. For the original model, the simulated temperatures of the canopy and the bare soil are represented by the average skin temperature.

The surface temperature is dominated by the bare ground component since the fraction of vegetation area was less than 15% at all times (Fig. 3a). However, the impact of the new temperature scheme on the total evaporation rate (Fig. 3c) is significant, and a reduction of almost 50% is caused by adopting the new scheme. The reduction of the evaporation is associated with a reduction of the canopy temperature by up to  $15^\circ\text{C}$ , closely matching the observations (Fig. 3b). Owing to the low absolute values of total evaporation, its strong relative reduction is balanced by only a slight increase of the sensible heat flux, consistent with a closed surface energy balance. The total soil heat flux is hardly

affected by the new parameterization (figures not shown).

The significance of the modification on the timescale of the full 60-day period is evident for the cumulative evaporation, shown in Fig. 4. In contrast to the FIFE simulation, the differences between the model formulations result in a significantly different total amount of water extracted from the soil reservoir, nearly 15 mm. The VB95 surface scheme produces a large overestimation in particularly the first half of the period. Later on, the difference between the two schemes reduces, and also the new scheme overestimates the measured evaporation. This feature is strongly related to the empirical nature of the formulation of the canopy resistance and the vegetation coverage  $C_v$ . However, the impact of the isothermal treatment of the surface as by VB95 is clearly demonstrated in Fig. 4.

#### 4. The numerical value of the skin conductivity

In the model of VB95, the apparent skin conductivity  $\Lambda$  is defined as the heat flux through the vegetation layer per degree temperature difference between the skin layer and the upper soil layer [namely Eq. (2)]. For calculations on the global scale, VB95 treat  $\Lambda$  as a fixed coefficient, with a value of  $7 \text{ W m}^{-2} \text{ K}^{-1}$  (Beljaars and Betts 1992). However, considerably different values may be expected for different types of surfaces.

For densely vegetated canopies, the value of  $\Lambda$  includes the heat conductivity of the canopy elements, the air within the canopy layer, and the top soil layer. Complicated processes as aerodynamic transport within the canopy layer and heat conduction through the stems inhibit an easy quantitative assessment of  $\Lambda$ . However, since the presence of the vegetation will thermally insulate the soil from the atmosphere,  $\Lambda$  may be expected to be small.

On the other hand, when vegetation is sparse or absent, the skin temperature is dominated by the (underlying) soil. In that case, the temperature difference appearing in (2) is proportional to the soil temperature gradient immediately below the surface, which may be significant, especially for dry soils. Equation (2) can then be compared to an ordinary conductivity equation for soil heat flow of the form

$$G = -\Lambda \Delta T = -(\Lambda \Delta z) \frac{\Delta T}{\Delta z} \approx -\lambda \frac{\partial T}{\partial z}. \quad (8)$$

From this equation, the apparent heat conductivity  $\Lambda$  can be interpreted as a physical conductivity by multiplication with a reference depth. The temperature difference defined by (2) can be treated as a real gradient by division by the same depth. Thus, for bare soils  $\Lambda \Delta z$  is proportional to the soil thermal conductivity  $\lambda$ , which depends on type and moisture content of the top soil.

A similar approach was followed by Mahrt and Pan (1984), who chose  $\Delta z$  to be the center of the model top soil layer, that is,  $z_1/2$ . In cases of steep nonlinear

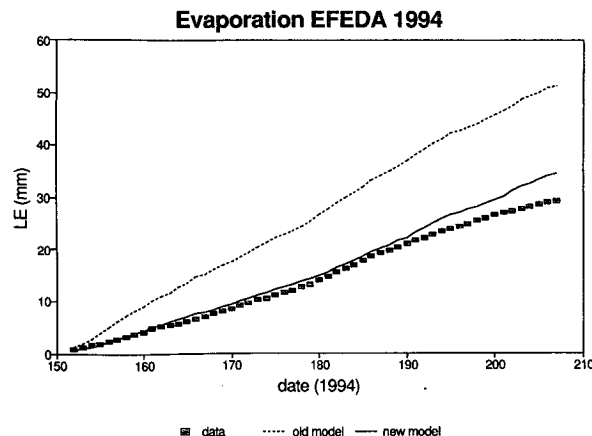


FIG. 4. Simulated and observed cumulative evaporation for the EFEDA 1994 simulation. Symbols as in Fig. 3.

temperature gradients near the surface, significant truncation errors are introduced when  $z_1$  is chosen too large. Therefore, a better choice for  $\Delta z$  would be the depth where the real temperature profile equals the temperature of the model top soil layer  $T_1$ . In principal this will not be a constant depth. At times where the soil heat flux density is large, steep temperature profiles with an exponential shape are present, and  $\Delta z$  is expected to be smaller than  $z_1/2$ .

The EFEDA dataset, described above, provides a useful test case to determine a value for  $\Lambda$  for a typical Mediterranean sparse canopy surface. Simulations of soil heat flux density were carried out using the modified scheme, in which soil physical and aerodynamic parameters were selected as before, and the surface temperature of each fraction was found by a separate solution of the energy balance for each fraction. In order to examine the effects of the choice for  $\Lambda$  in the modified ECMWF scheme, sensitivity experiments were carried out with four different values of  $\Lambda$  for the bare soil component, namely, 7, 14, 17, and  $21 \text{ W m}^{-2} \text{ K}^{-1}$ . The value of  $\Lambda$  was kept at the suggested value of  $7 \text{ W m}^{-2} \text{ K}^{-1}$  for the gridbox fractions covered with vegetation and the interception reservoir.

Figure 5 shows the simulated and measured soil heat flux  $G$  for the same days as presented above, that is, six consecutive days in the center of the period. For daytime situations ( $G > 0$ ), the default value of  $7 \text{ W m}^{-2} \text{ K}^{-1}$  yields an average underestimation of  $G$  of approximately 26% (regression coefficient  $R^2 = 0.73$ ). Here  $\Lambda = 21 \text{ W m}^{-2} \text{ K}^{-1}$  gives a small overestimation (5%, with  $R^2 = 0.81$ ), while for  $\Lambda = 14 \text{ W m}^{-2} \text{ K}^{-1}$  the simulation is slightly improved (4% too low,  $R^2 = 0.86$ ). An optimal simulation is carried out by taking an intermediate value for  $\Lambda = 17 \text{ W m}^{-2} \text{ K}^{-1}$  (no average difference,  $R^2 = 0.84$ , curve not shown in Fig. 5). As a consequence of the surface energy balance equation, the sensible and latent heat fluxes are reduced

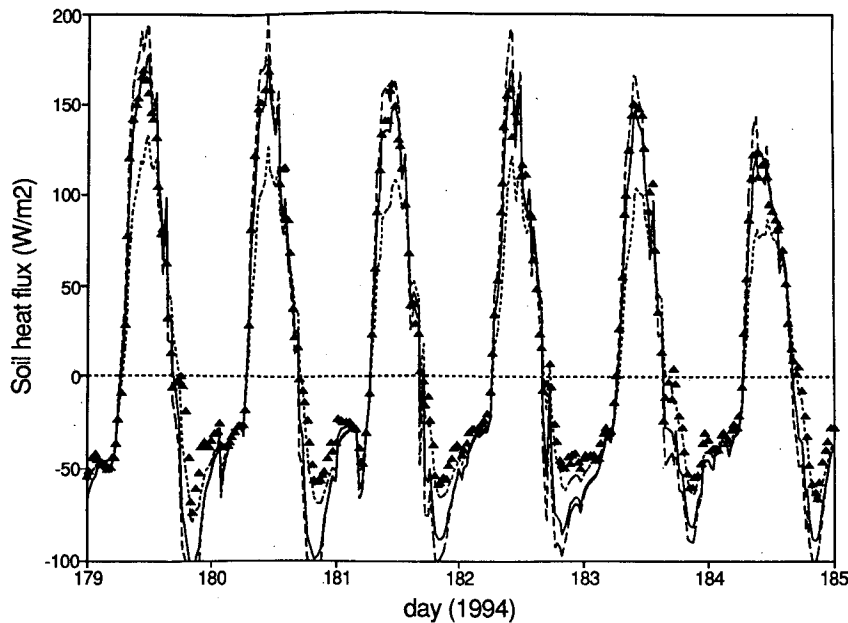


FIG. 5. Measured (symbols) and simulated (lines) values of the soil heat flux for a series of days in the EFEDA 1994 case. Simulations include  $\Lambda = 7$  (dotted line), 14 (solid line), and 21 (dashed line)  $\text{W m}^{-2} \text{K}^{-1}$ .

by several tens of watts per square meter at most when  $\Lambda$  is increased from 7 to 21  $\text{W m}^{-2}$ . For nighttime values ( $G < 0$ ), the higher values of  $\Lambda$  result in larger discrepancies from the observations. However, data quality of nighttime observations is somewhat uncertain, and a sufficient energy balance closure was systematically not reached.

## 5. Discussion and conclusions

This paper considers two simplifications applied in the new ECMWF surface scheme: a uniform skin-layer temperature and a constant value of the skin-layer conductivity for all surface types.

A new treatment of the surface temperature is proposed, which has a better physical basis than the isothermal assumption adopted by VB95. A simple scheme is presented to allow the different surface fractions (bare soil, dry vegetation, and an interception reservoir) to adopt temperatures that are in equilibrium with their state of evaporation, as in the Penman–Monteith concept (Monteith 1965). The three surface temperatures are solved according to the original scheme by first regarding each of the fractions as if fully covering the grid box and then averaging the resulting fluxes and surface temperatures using a similar weighting as used for the evaporation (5). By initializing each surface fraction energy balance solution using the average skin temperature from the previous time step and employing a second iteration to minimize the error involved with linearization of  $\partial q_{\text{sat}}/\partial T$  and the stability

dependence of  $C_H$ , no additional information needs to be stored between subsequent time steps. Hence, the proposed modification of the surface scheme can be implemented without a severe change of the model infrastructure. In the appendix this numerical scheme is shown to have virtually identical results as a full iteration for each surface fraction energy balance.

This procedure is somewhat different from the dual source models presented by, for example, Deardorff (1978), Shuttleworth and Wallace (1985), or Choudhury and Monteith (1988). In their models, an interaction between the bare soil and vegetation takes place directly by computing a temperature and humidity deficit within the canopy layer and computing fluxes from either of these components through this canopy-layer node. Blyth (1995) presented a more general concept by placing this node at some level between the surface and the lowest model layer, which serves as a reference height for the surface forcings.

A major disadvantage of this concept for large-scale meteorological models is the data requirement. The values of the resistances between this node and the various surface fractions need to be parameterized and cannot be expected to be of similar magnitude for all vegetation types or degrees of coverage (McNaughton and Van den Hurk 1995). In the current ECMWF scheme, the aerodynamic transfer between the surface and the reference level allows no direct interaction between various surface fractions since the fluxes from each component are treated as purely additive. However, in a surface-layer model coupled to a model for



the rest of the atmosphere, the surface fluxes will affect the meteorological forcings at the reference height via boundary layer interaction. This feedback serves as an indirect interaction mechanism between the surface fractions.

The new scheme considerably altered the partitioning of latent heat flux over the vegetation and the soil, in a case study where the behavior of a drying vegetated surface wetted by rain was simulated. In the original scheme, maximum soil evaporation was of the same order as the canopy evaporation, in spite of the fact that only 15% of the surface was not vegetated. The new scheme reduced the soil evaporation by 50% and enhanced the canopy evaporation slightly. In the FIFE dataset, the frequency of rain events followed by wet soil evaporation is not high, and the accumulated evaporation calculated for 168 consecutive days by the original and the modified scheme differed by only 5 mm. The difference between the surface temperatures of the soil and vegetation components is usually rather small since the top soil layer usually remains wet enough to sustain soil evaporation. Assuming these temperatures to be equal has only a limited impact during most occasions.

By contrast, a case study carried out using a dataset collected over a sparsely vegetated dry vineyard with negligible soil evaporation showed a significant reduction of the canopy evaporation when the original scheme of VB95 was replaced by the modified version. The simulations of total evaporation carried out with the new scheme matched observations rather well, while the original scheme caused an overestimation of approximately 75% throughout the entire simulation period of 60 days. Obviously, the formulation of the canopy resistance  $r_c$  and the vegetation coverage  $C_v$  are strongly linked to the simulation of evaporation. A similar change of the simulated canopy evaporation could also have been obtained by optimizing these parameters. However, it merely is the purpose of this paper to show the effect of the assumption of the uniform surface temperature used by VB95, rather than to verify all components of their model. The distinction of different surface temperatures is physically more realistic and is shown to have a significant impact on the canopy evaporation.

In general, solution of the surface temperature for separate surface components reduces evaporation of those components that are cooler than their surroundings. In the FIFE dataset, the soil evaporation was significantly reduced, whereas evaporation by the vegetation was reduced for the Spanish simulation.

Also the parameterization of the soil heat flux by use of a skin conductivity  $\Lambda$  assumed constant for all vegetation types, was evaluated using data collected during EFEDA 1994. It was shown that for a bare soil surface,  $\Lambda$  is proportional to the soil thermal conductivity  $\lambda$ . The coefficient of proportionality is a reference depth  $\Delta z$ . Mahrt and Pan (1984) proposed to choose  $\Delta z$  as the

center of the top soil layer, but for steep nonlinear temperature gradients this depth may be chosen closer to the surface.

For the dry Mediterranean vineyard, soil temperature and soil heat flux data showed that  $\Lambda = 17 \text{ W m}^{-2} \text{ K}^{-1}$  is a better estimate than the presumed value of  $7 \text{ W m}^{-2} \text{ K}^{-1}$ . For this case, the thermal conductivity of the upper soil levels was estimated to be  $0.3 \text{ W m}^{-1} \text{ K}^{-1}$  (Verhoef et al. 1996). Using  $\Lambda = 17 \text{ W m}^{-2} \text{ K}^{-1}$ ,  $\Delta z$  would be approximately 1.8 cm.

The value of  $\Lambda = 7 \text{ W m}^{-2} \text{ K}^{-1}$  was obtained from soil heat flux densities observed at a meadow grassland site near Cabauw, the Netherlands (Beljaars and Betts 1992). The difference with the value found from the EFEDA 1994 data is presumably associated with the different insulation properties of the vegetation types at both sites. While the sparse vineyard canopy had a low degree of vegetation cover (<15%), hardly providing a barrier for heat transfer between the soil and the atmosphere, the grass vegetation near Cabauw more effectively insulated the underlying soil.

The two values found for  $\Lambda$  possibly mark the likely range of values for most surface types. Based upon the physical arguments for the value of  $\Lambda$ , an adequate strategy is to calculate the soil heat flux by using  $\Lambda = 7 \text{ W m}^{-2} \text{ K}^{-1}$  for the vegetated part of the grid box and the higher value of  $17 \text{ W m}^{-2} \text{ K}^{-1}$  for the bare-soil part. The strategy provides a considerable improvement of the physical basis of the current parameterization of  $G$ . The simple interpolation as proposed here requires no new global input and is easily implemented in the present ECMWF surface scheme.

*Acknowledgments.* We are grateful to our colleagues from the Winand Staring Centre in Wageningen and the University of Copenhagen for the pleasant collaboration during the EFEDA experimental period. We wish to thank Henk de Bruin, Pedro Viterbo, and Anne Verhoef for their valuable comments. We also thank Alan Betts for making the FIFE 1987 data available. Three anonymous referees raised valuable comments on an earlier version of the manuscript. BvdH was supported by the Dutch NWO under Contract 762-365-030 and by the EC under Contract EPOC CT90-0030.

#### APPENDIX

##### Effect of the Number of Iterations on the Energy Balance Solution

The model of VB95 uses the value of the skin temperature and the sensible heat flux density from the previous time step to linearize  $\partial q_{\text{sat}}/\partial T$  and to calculate the stability dependence of  $C_H$ , respectively. In the modified version,  $T_s$  and  $H$  are calculated for each grid-box fraction separately, and intermediate storage of these parameters between subsequent time steps was to be avoided. When the surface temperatures of the different grid-box fractions differ significantly, a

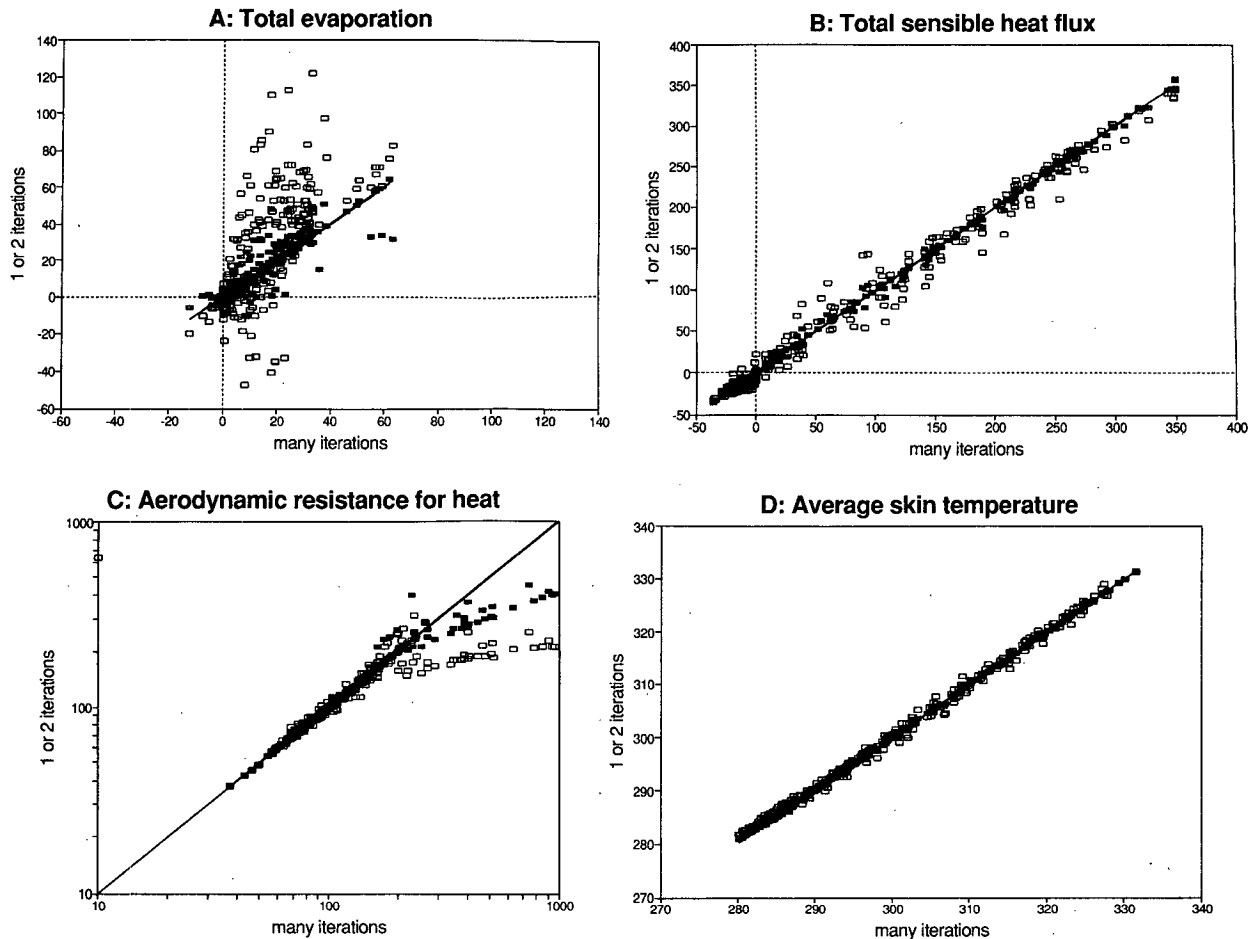


FIG. A1. EFEDA simulations of (a) total evaporation, (b) total sensible heat flux, (c) aerodynamic resistance, and (d) average skin temperature, computed by means of a fully iterative scheme for each surface fraction ( $x$  axis) and with 1 ( $\square$ ) and 2 ( $\blacksquare$ ) iterations only ( $y$  axis).

(weighted) average skin temperature from the previous time step will introduce significant errors in the estimation of  $q_{\text{sat}}$ . Obviously, similar errors are introduced if a linearization around the reference temperature is carried out and the surface temperature differs significantly from this value (McArthur 1990). A similar argument can be put forward for the stability function in  $C_H$  when the sensible heat flux densities from the various surface components differ considerably. An iteration procedure of (1)–(7) is necessary to find appropriate values of  $\partial q_{\text{sat}}/\partial T$  and  $C_H$ . This is a rather expensive procedure in an operational weather forecast system and for that reason the number of iterations was limited to two in the calculations shown above.

During the EFEDA case, occasions with large temperature differences between the canopy and bare soil fraction often occurred. Therefore, this is a good case to test the effect of numerical approximations outlined previously. We compare one, two, and many iterations (until full convergence).

Figure A1 show the results in terms of simulated total evaporation (Fig. A1a), total sensible heat (Fig. A1b), aerodynamic resistance  $r_a$  (Fig. A1c), and skin temperature (Fig. A1d). A clear difference is present between 1 and 2 iterations, especially for the simulated latent heat flux. The deviations are particularly large for relatively low values of LE that occur just after sunrise and before sunset when the rate of change of the surface temperature is large. Smaller deviations are present for the sensible heat and skin temperature.

With two iterations, the total evaporation, sensible heat, and skin temperature agree very well with the fully iterative solution.

#### REFERENCES

- Beljaars, A. C. M., 1992: Numerical schemes for parameterizations; ECMWF seminar proceedings, September 1991. *Numerical Methods in Atmospheric Models*, ECMWF, 1–42.
- , and A. A. M. Holtslag, 1991: Flux parameterization over land surfaces for atmospheric models. *J. Appl. Meteor.*, **30**, 327–341.

- , and A. K. Betts, 1992: Validation of the boundary layer scheme in the ECMWF model; ECMWF seminar proceedings 7–11 September 1992. *Validation of Models Over Europe*. Vol. II. ECMWF, 159–195.
- Betts, A. K., and J. H. Ball, 1992: FIFE-1987 mean surface time series. Data diskette, Atmospheric Research.
- Blyth, E. M., 1995: Using a simple SVAT-scheme to describe the effect of scale on aggregation. *Bound.-Layer Meteor.*, **72**, 267–285.
- Bolle, H. J., and Coauthors, 1993: EFEDA: European field experiment in a desertification threatened area. *Ann. Geophys.*, **11**, 173–189.
- Choudhury, B. J., and J. L. Monteith, 1988: A four-layer model for the heat budget of homogeneous land surfaces. *Quart. J. Roy. Meteor. Soc.*, **114**, 373–398.
- Deardorff, J. W., 1978: Efficient prediction of ground surface temperature and moisture, with inclusion of a layer of vegetation. *J. Geophys. Res.*, **83**, 1889–1903.
- Dolman, A. J., 1993: A multiple-source land surface energy model for use in general circulation models. *Agric. For. Meteorol.*, **65**, 21–45.
- Mahrt, L., and H. Pan, 1984: A two-layer model of soil hydrology. *Bound.-Layer Meteorol.*, **29**, 1–20.
- McArthur, A. J., 1990: An accurate solution to the Penman equation. *Agric. For. Meteorol.*, **51**, 87–92.
- McNaughton, K. G., and B. J. J. M. van den Hurk, 1995: A 'Lagrangian' revision of the resistors in the two-layer model for calculating the energy budget of a plant canopy. *Bound.-Layer Meteorol.*, **74**, 261–288.
- Monteith, J. L., 1965: Evaporation and the environment. *Symp. Soc. Exp. Biol.*, **19**, 205–234.
- , 1981: Evaporation and surface temperature. *Quart. J. Roy. Meteor. Soc.*, **107**, 1–27.
- Noilhan, J., and S. Planton, 1989: A simple parameterization of land surface processes for meteorological models. *Mon. Wea. Rev.*, **117**, 536–549.
- Sellers, P. J., F. G. Hall, G. Asrar, D. E. Strebel, and R. E. Murphy, 1988: The first ISLSCP field experiment (FIFE). *Bull. Amer. Meteor. Soc.*, **69**, 22–27.
- Shuttleworth, W. J., and J. S. Wallace, 1985: Evaporation from sparse crops—An energy combination theory. *Quart. J. Roy. Meteor. Soc.*, **111**, 839–855.
- van den Hurk, B. J. J. M., 1996: Sparse canopy parameterizations for meteorological models. Ph.D thesis, Wageningen Agricultural University, 271 pp.
- , A. Verhoef, A. van den Berg, and H. A. R. de Bruin, 1995: An intercomparison of three vegetation/soil models for a sparse vineyard canopy. *Quart. J. Roy. Meteor. Soc.*, **121**, 1867–1889.
- Verhoef, A., B. J. J. M. van den Hurk, A. F. G. Jacobs, and B. G. Heusinkveld, 1996: Thermal soil properties for a vineyard (EFEDA-I) and a savanna (HAPEX-SAHEL). *Agric. For. Meteorol.*, **78**, 1–18.
- Viterbo, P., and A. C. M. Beljaars, 1995: An improved land surface parameterization scheme in the ECMWF model and its validation. *J. Climate*, **8**, 2716–2748.